

Nanoparticles 2009

University of Liverpool

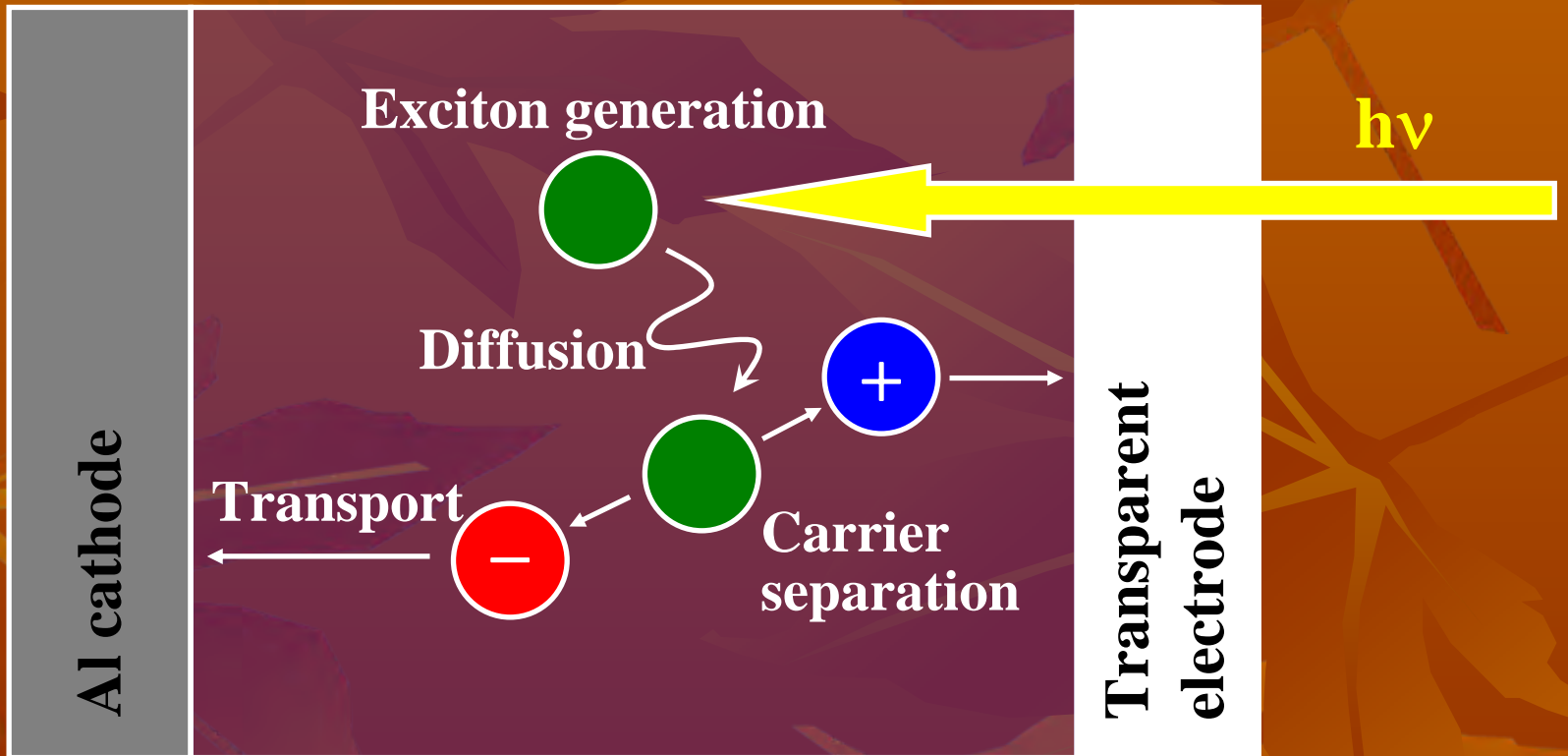
4 Sep 2009

**Printable photovoltaics
using colloidal quantum dots**

Shinya Maenosono

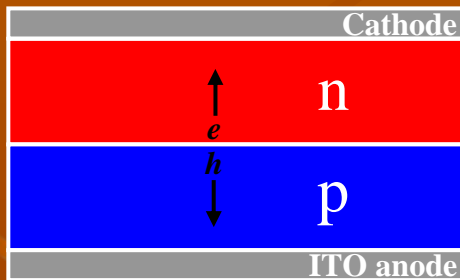
Japan Advanced Institute of Science and Technology

Elementary steps in OPVCs

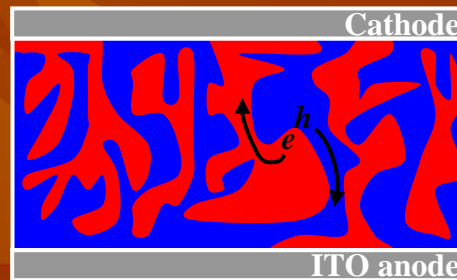


Advancement of device structure

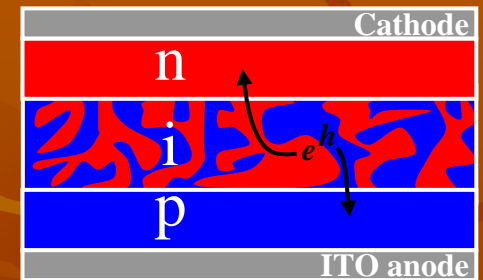
Flat heterojunction
(FHJ)



Bulk heterojunction
(BHJ)



p-i-n structure



i: intrinsic

Introduce a *p-n* junction

Increase the interfacial area between *p* and *n* phases
Secure carrier transport pathways for *e* and *h*

Block undesirable transport of *e* and *h*

BHJ devices fabricated by blending C₆₀ derivatives

Photoinduced electron transfer from **a conjugated polymer** to **a methanofullerene** occurs on a timescale of 50 fs, whereas the timescale for back transfer is very long.

Once this metastable charge-separated state is formed, the free charges are transported through the device through diffusion and drift processes.

The latter is induced by using top and bottom electrodes that have different work-functions, thus providing a built-in potential over the active layer.

In the active layer, holes are transported through **the conjugated polymer matrix**, and electrons are transported by hopping between **fullerene molecules**.

Conventional QDSCs

As **an acceptor material**, wide-gap semiconductor (e.g., CdSe and InP) QDs have widely been used.

As **a donor material**, conjugated polymers (e.g., MEH-PPV and P3HT) have usually been used, because they can be solution-processed and are compatible with QDs.

Problems

Wide-gap semiconductor QDs have very little absorption at infrared (IR) wavelengths.

However, the conjugated polymers have low carrier drift mobility (μ) and they are usually easily degraded.

Our strategy

Acceptor

PCBM (fullerene derivative) or wide-gap semiconductor QDs



Narrow-gap IV-VI QDs



Donor

Conjugated polymer (e.g. P3HT)

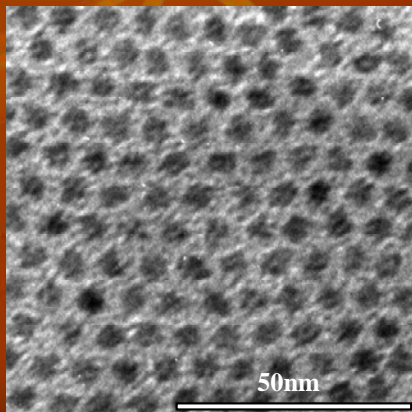
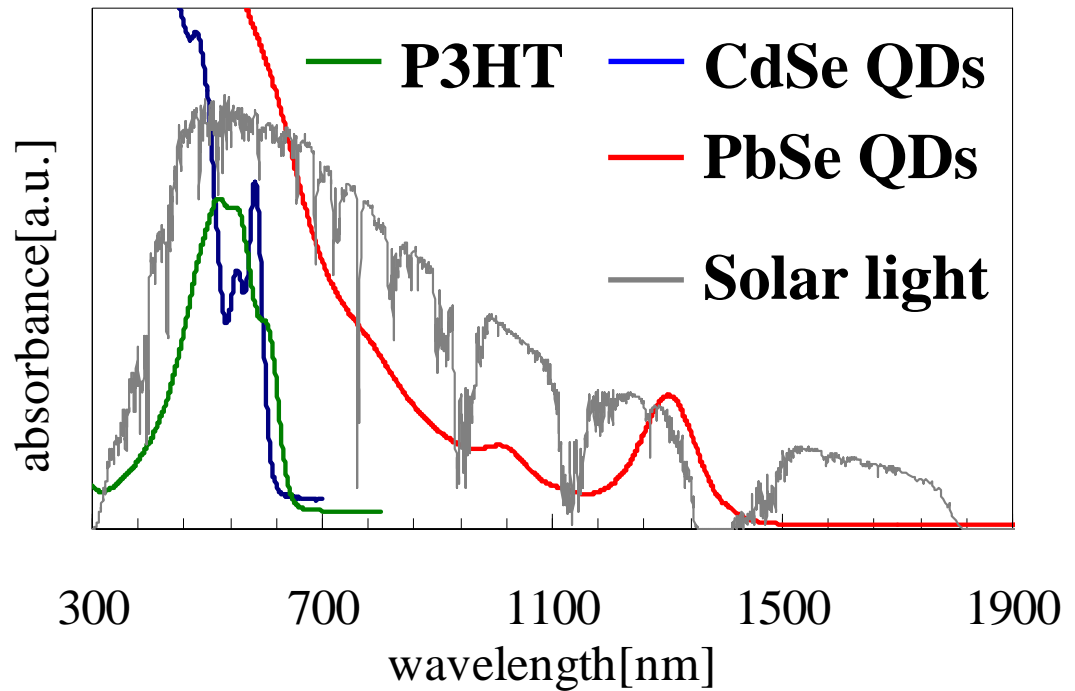
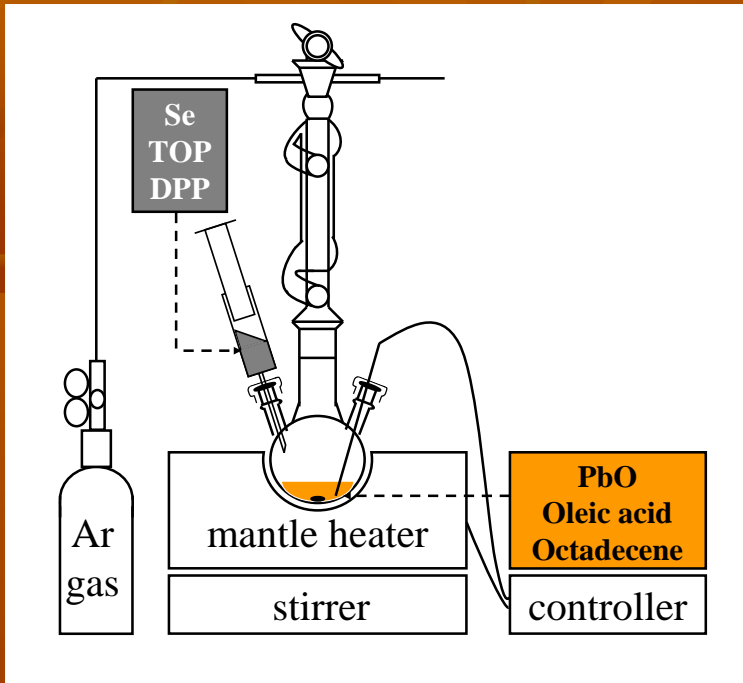


Low-Mw crystalline organic semiconductor



To solve the conventional problems

Narrow-gap PbSe QDs



$D_p = 4.7 \text{ nm}$
 $\sigma = 8 \%$

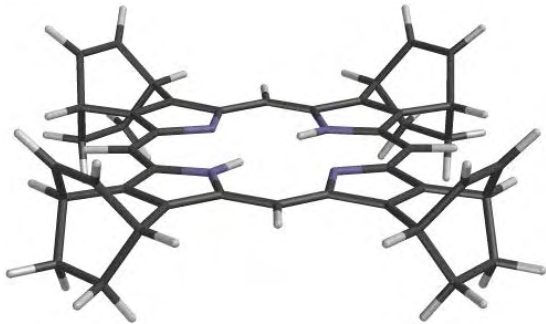
PbSe QDs are expected to be good candidates as **acceptor materials** in BHJ solar cells to improve the coverage of the solar spectrum.

High efficiency carrier multiplication

PbSe QDSC is thought to attain maximum η up to 60% due to carrier multiplication.

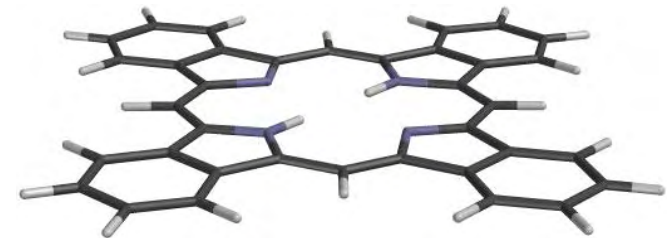
Organic semiconductor

Tetrabenzoporphyrin (BP)



Soluble but insulator

Anneal



Insoluble but semiconductor

Mobility: $\mu_{\text{FET}} \sim 0.1 \text{cm}^2 \text{V}^{-1} \text{s}^{-1}$

S. Aramaki et al., Appl. Phys. Lett. **84**, 2085(2004)

By changing the organic matrix from a polymer to a low-molecular-weight material



High conversion efficiency and high durability

Summary of strategy

Acceptor

PCBM (fullerene derivative) or wide-gap semiconductor QDs



PbSe QDs

Improvement of the coverage of the solar spectrum

Carrier multiplication

High drift mobility ($\sim 0.8 \text{ cm}^2 \text{ V}^{-1} \text{ S}^{-1}$)



Donor

Conjugated polymer (e.g. P3HT)



Tetrabenzoporphyrin (BP)

Solution processable

High durability due to high crystallinity

High drift mobility ($\sim 0.1 \text{ cm}^2 \text{ V}^{-1} \text{ S}^{-1}$)

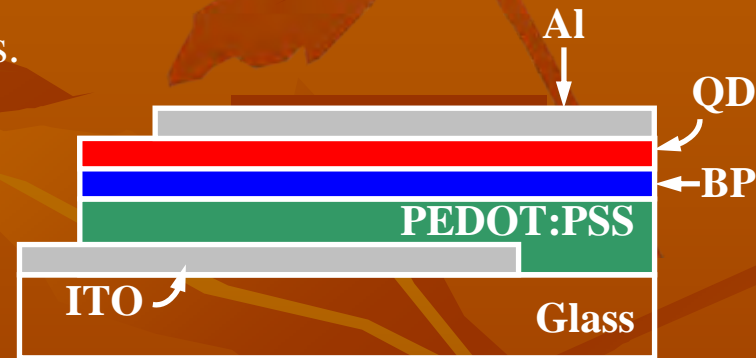


Combine these two materials with great potential

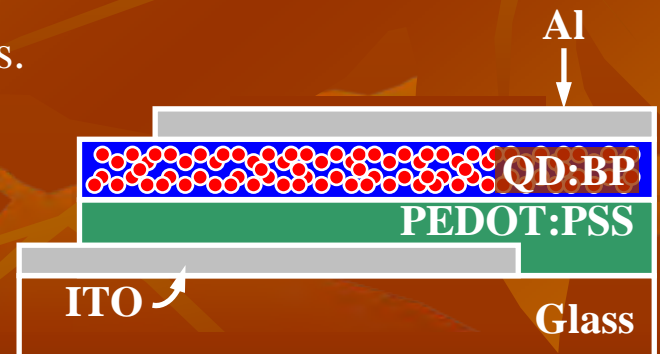
Device fabrication

A buffer layer of poly(3,4-ethylenedioxythiophene):poly(styrenesulfonate) (PEDOT:PSS) (100 nm thick) was coated on the ITO anodes, and baked at 150 °C for 30 min under N₂.

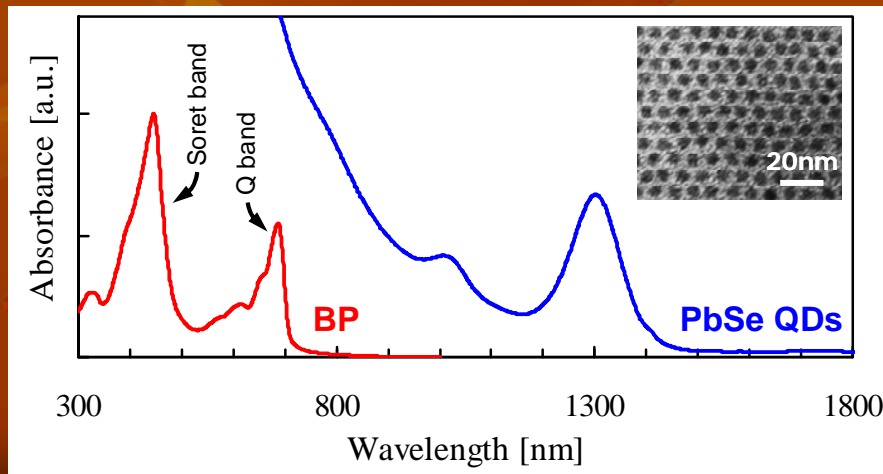
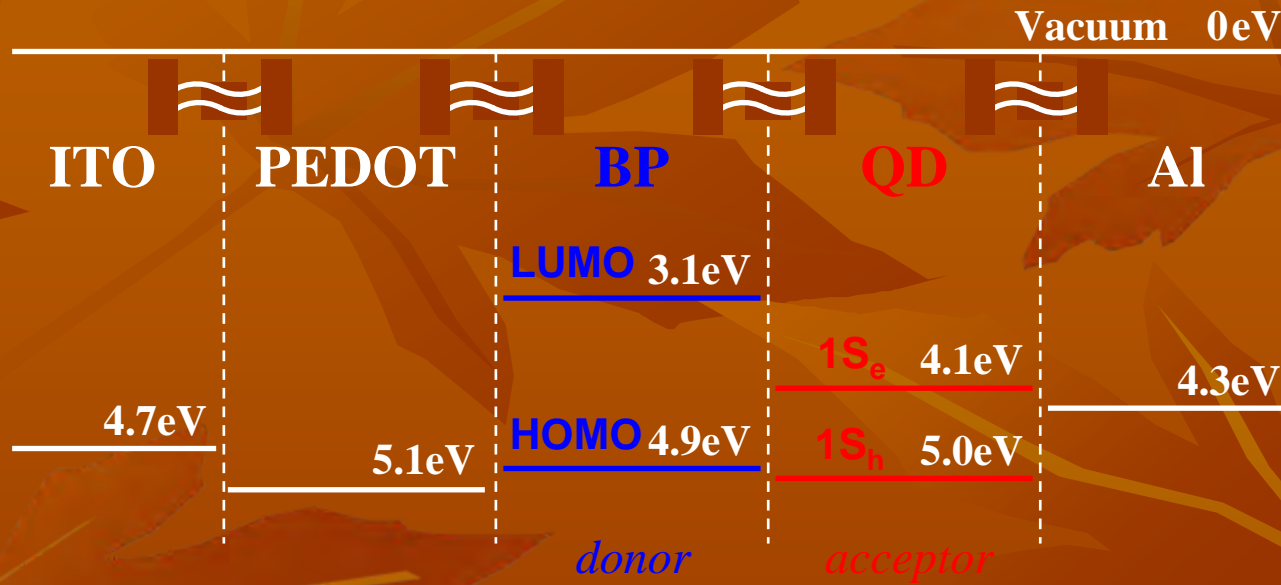
The FHJ structure (BP/QD) was fabricated as follows. First, a chloroform solution of CP was spin coated on the PEDOT:PSS layer. It was then annealed at 200 °C for 20 min under N₂ to transform CP to BP (50 nm thick). Secondly, a chloroform dispersion of PbSe QDs was spin cast onto the BP film (50 nm thick). Finally, an Al cathode (100 nm thick) was fabricated on the QD layer *via* vacuum deposition.



The BHJ structure (BP:QD) was fabricated as follows. A chloroform solution of CP and QDs (40:60, vol:vol) was spin coated on the PEDOT:PSS layer. It was then annealed at 200 °C for 20 min under N₂.



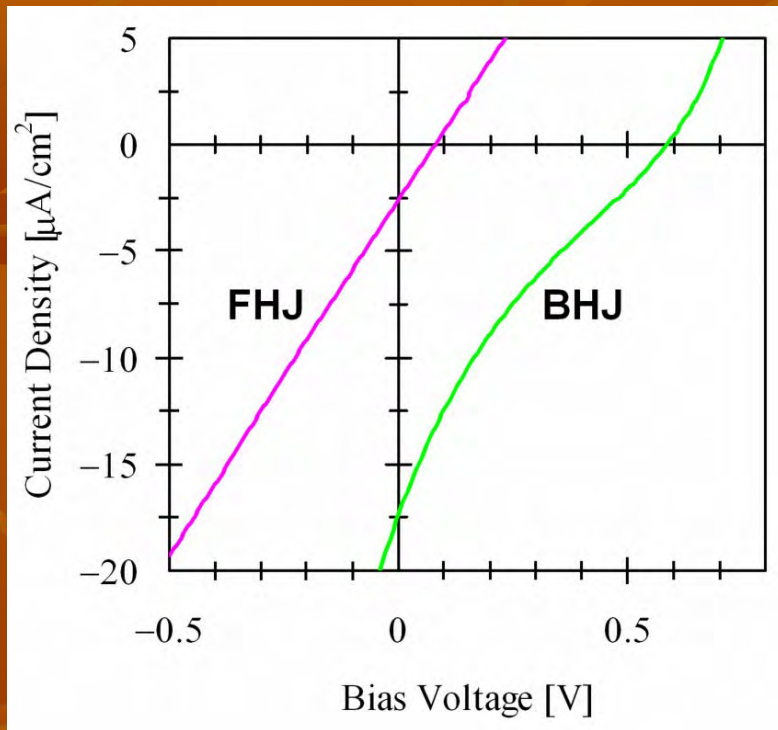
Energy diagram



The HOMO level of BP and the $1S_h$ level of the QDs were measured using a photoelectron spectrometer.

The LUMO level of BP and the $1S_e$ level of the QDs were estimated from peaks of the *Q* band and the first exciton absorption, respectively.

Photovoltaic conversion



For the first time, we succeeded to fabricate the polymer-free QDSCs, which can operate with IR light, using PbSe QDs and BP *via* a solution process.

Energy conversion efficiency

Our BHJ device

$1.8 \times 10^{-3}\%$

under 800-nm NIR illumination ($100 \text{ mW}\cdot\text{cm}^{-2}$)

Appl. Phys. Lett. **92**, 173307 (2008)

PbSe/P3HT device

0.14%

under AM1.5G illumination ($100 \text{ mW}\cdot\text{cm}^{-2}$)

D.H. Cui *et al.*, *Appl. Phys. Lett.* **88**, 183111 (2006)

PbSe/(P3HT:pentacene) device

$1.8 \times 10^{-4}\%$

under AM1.5G illumination ($60 \text{ mW}\cdot\text{cm}^{-2}$)

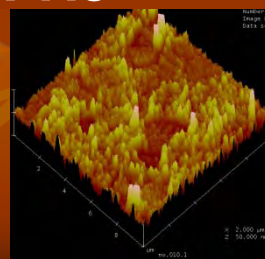
R. Thapa *et al.*, *Appl. Phys. Lett.* **90**, 252112 (2007)

Conceivable explanations for the low photovoltaic performance

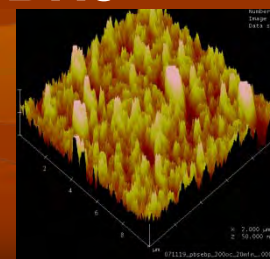
- (1) The small band offset between the HOMO level of BP and $1S_h$ level of PbSe QDs hinders hole injection from QDs to BP.
- (2) There is poor electrical contact between QDs and BP (or between QDs) due to the existence of ligand molecules on QD surfaces and/or low affinity between QDs and BP.
- (3) There is low crystallinity and hence low μ of the BP matrix due to an inhibition of crystallization by QDs.
- (4) The device has a low rectifying property probably due to the direct contact between BP and Al cathode caused by the roughened surface of the active layer.

The right figures show surface morphologies ($10 \times 10 \mu\text{m}^2$) of pure BP and BP:QD composite layers, taken by AFM.

FHJ



BHJ

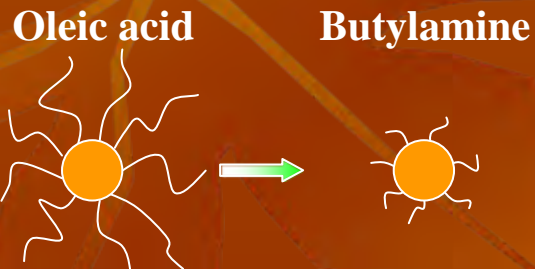


Ideas for the improvement of the photovoltaic performance

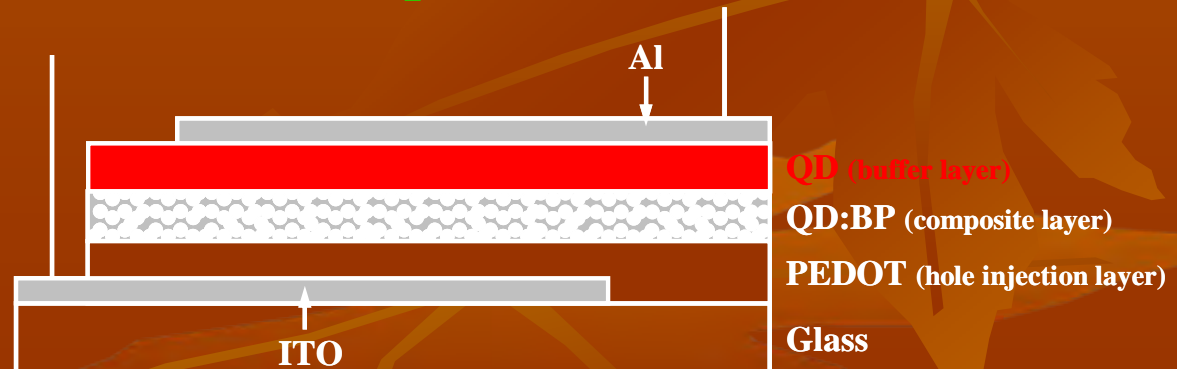
We exchanged the oleic acid surface ligands for butylamine ligands to improve the electrical contact between the QDs and BP, and introduced a buffer layer consisting of PbSe QDs onto the composite layer (BP:QD) to avoid the direct contact between BP and the Al cathode.

In addition, the QD buffer layer was treated with ethylenediamine to crosslink the PbSe QDs and increase the conductivity of the buffer layer.

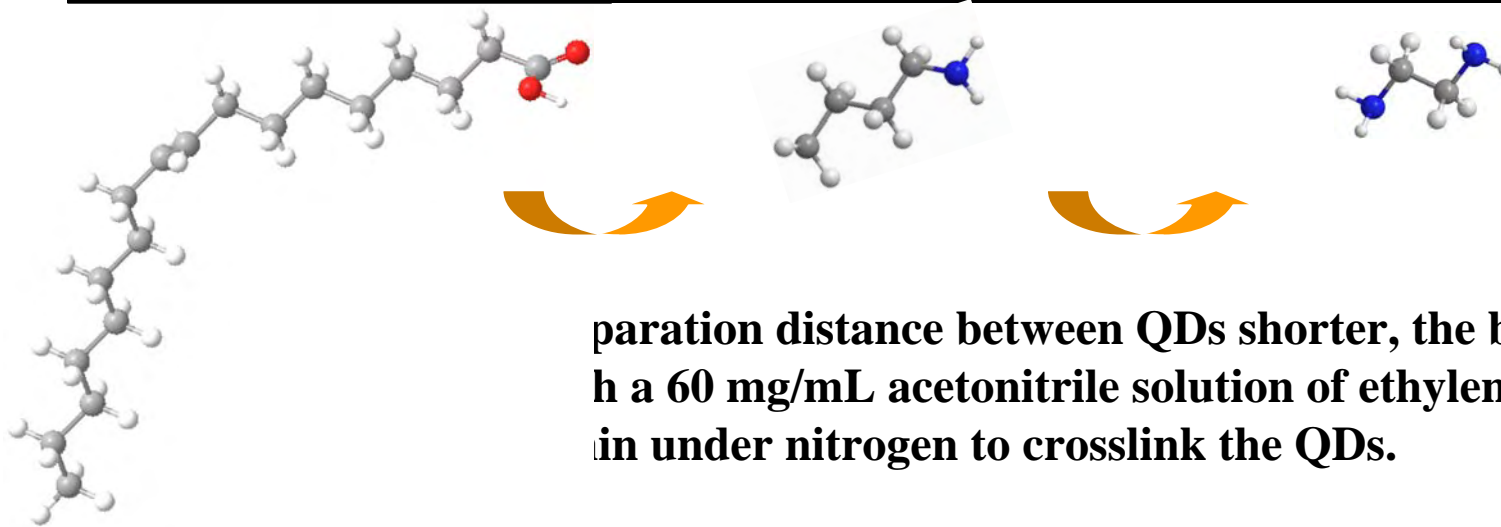
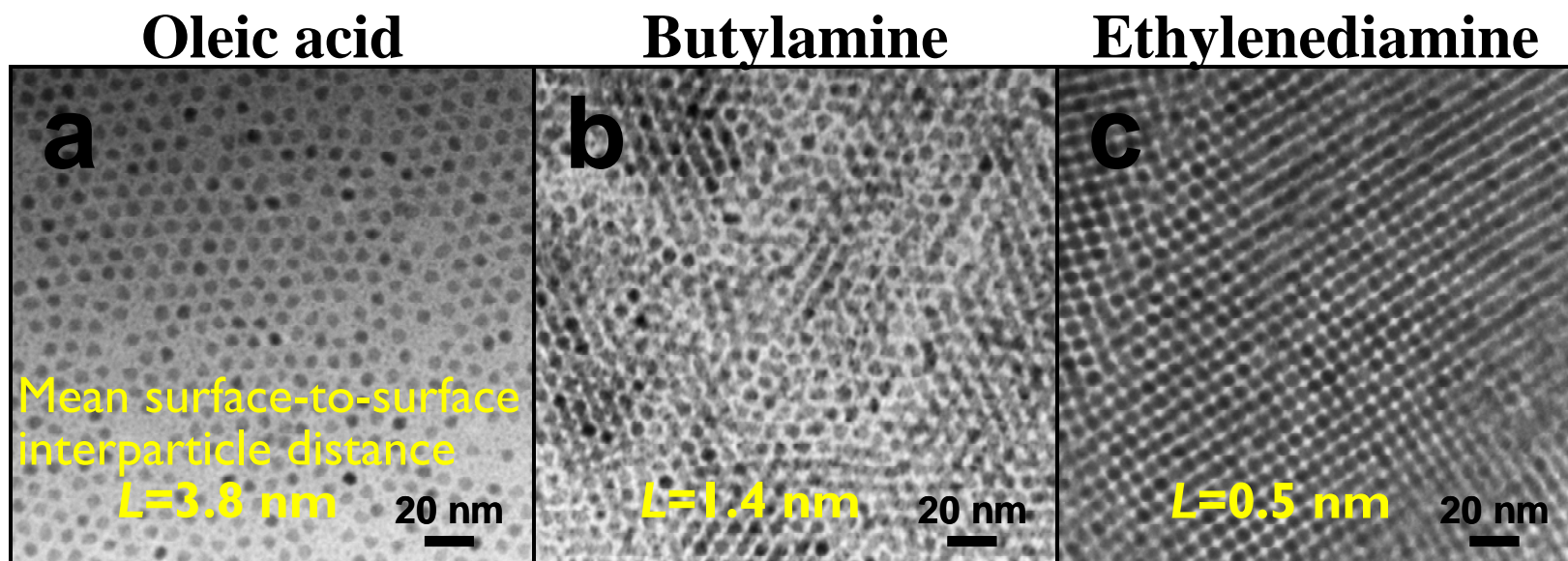
Ligand exchange



Introduction of a buffer layer (p-i-n structure)



Ligand exchange of QDs

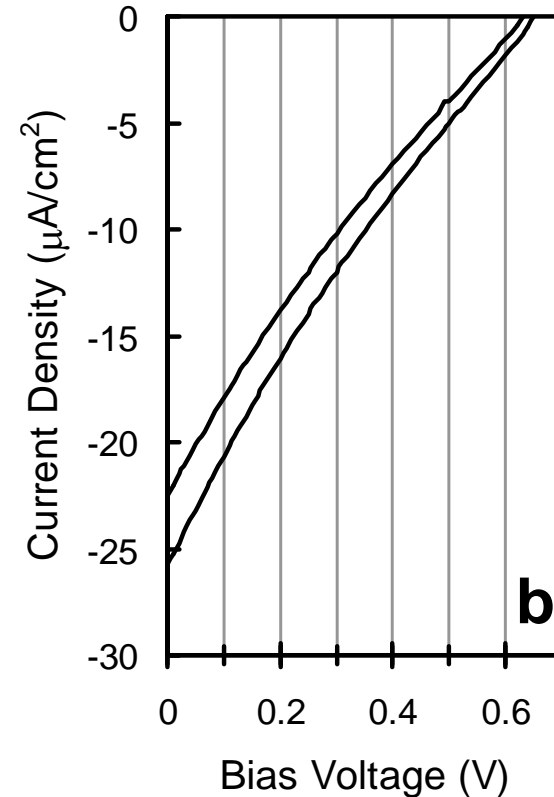
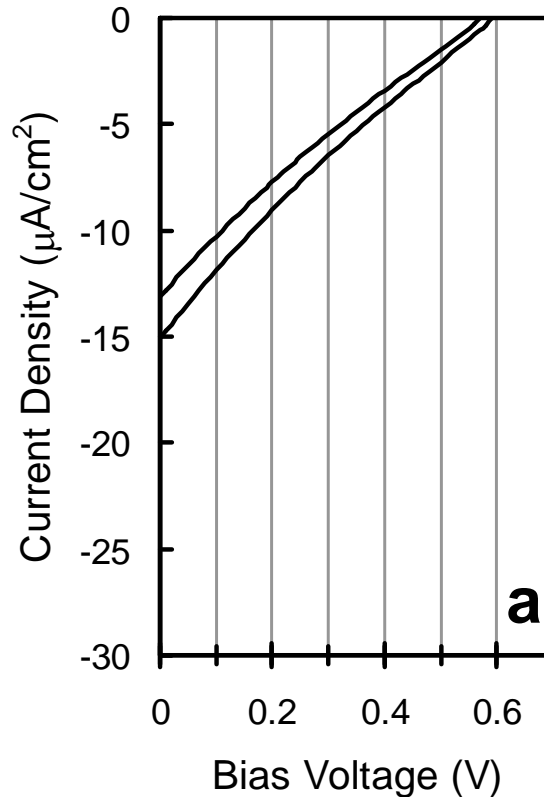


Photovoltaic conversion

ITO/PEDOT/BP:QD/**BA-capped QD**/Al

ITO/PEDOT/BP:QD/**EDA-linked QD**/Al

under 800-nm NIR illumination ($100 \text{ mW}\cdot\text{cm}^{-2}$)



To confirm that the results were reproducible, the J - V characteristics for two different samples, fabricated under the same conditions, were measured.

Short-circuit current density (J_{SC}): $13.1\sim 15.1 \mu\text{A cm}^{-2}$

Open-circuit voltage (V_{OC}): $0.57\sim 0.59 \text{ V}$

Fill factor (FF): **0.22**

Energy conversion efficiency (η): $1.6\sim 2.0 \times 10^{-3}\%$

J_{SC} : $22.5\sim 25.8 \mu\text{A cm}^{-2}$

V_{OC} : $0.63\sim 0.65 \text{ V}$

FF: **0.21~0.22**

η : $3.1\sim 3.5 \times 10^{-3}\%$

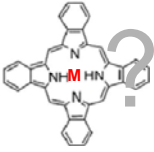
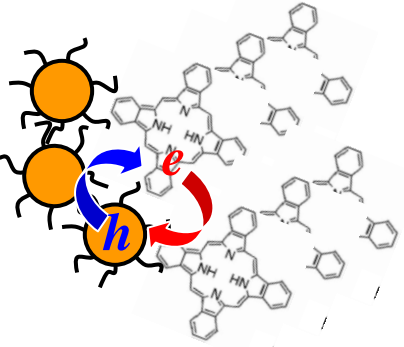
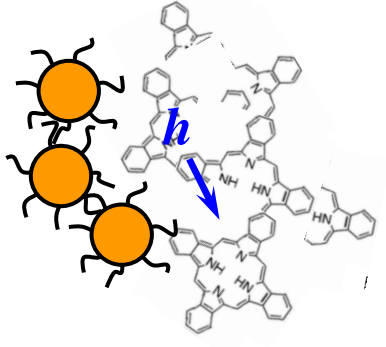
Discussion

J_{SC} of the EDA-treated device is 170% higher than that of the untreated device. On the other hand, V_{OC} of the EDA-treated device is only 110% higher than that of the untreated device. These results indicate that the EDA treatment of the buffer layer increases the quantum efficiency, while it does not significantly influence the built-in potential.

Hence, the improvement in J_{SC} observed in the EDA-treated device is likely due to an increase in the conductivity of the buffer layer from the decrease in the probability of carrier recombination and/or trapping.

Alternatively, the change in J_{SC} could be due to an improvement of the contact between the buffer layer and the Al electrode (or between the composite layer and the buffer layer), or be due to an improvement of the homogeneity of the active region.

Remaining issues

<p>BP</p> <p><u>LUMO 3.1eV</u></p> <p><u>HOMO 4.9eV</u></p>	<p>QD</p> <p><u>1S_e 4.1eV</u></p> <p><u>1S_h 5.0eV</u></p>			
--	--	---	--	---

The small band offset between the HOMO level of BP and 1S_h level of QDs

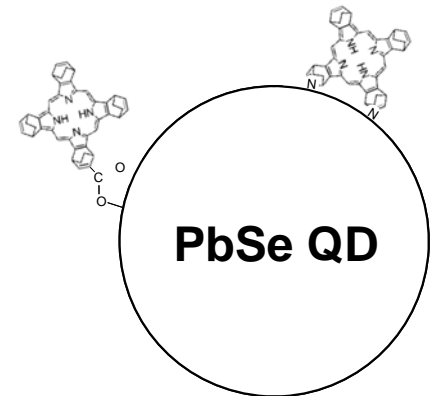
There is poor electrical contact between QDs and BP due to the existence of ligand molecules on QD surfaces.

There is low crystallinity and hence low μ of the BP matrix.

More essential problem

The lifetime of multi carrier is rather short (<50 ps).

How to extract holes from QD cores before Auger recombination ?



Conclusions

The polymer-free QDSCs, which can operate with IR light, were fabricated using PbSe QDs and BP *via* a solution process.

We observed photovoltaic conversion for the devices in the IR region and the energy conversion efficiency was found to be of the order of $10^{-3}\%$ under 100 mW cm^{-2} illumination at 800 nm.

The EDA treatment of QD buffer layer improves the energy conversion efficiency of the QDSCs. This is because the EDA-treatment decreases the surface-to-surface interparticle distance and improves J_{SC} of the device.

However, optimally balancing the crystallization of BP and BP-QD interfacial compatibility is a problem remaining to be solved.